Partial Differential Equations in Applied Mathematics 9 (2024) 100607

Contents lists available at ScienceDirect

Partial Differential Equations in Applied Mathematics

journal homepage: www.elsevier.com/locate/padiff

Laplace transform-homotopy perturbation method for fractional time diffusive predator–prey models in ecology

Kolade M. Owolabi [a,*], Edson Pindza [b], Berat Karaagac [c], Gulay Oguz [d]

[a] Department of Mathematical Sciences, Federal University of Technology Akure, PMB 704, Akure, Ondo State, Nigeria
[b] Department of Mathematics and Applied Mathematics, University of Pretoria, Pretoria 002, South Africa
[c] Faculty of Education, Department of Mathematics Education, Adiyaman University, Adiyaman, Turkey
[d] Department of Mathematics, Harran University, Sanliurfa, Turkey

ARTICLE INFO

MSC:
65L05
65M06
65N20
93C10

Keywords:
Subdiffusive predator–prey models
Linear stability analysis
Homotopy perturbation method
Simulations in 1D-2D

ABSTRACT

In this paper, we consider some reaction–diffusion systems arising from two-component predator–prey models with various kinetics ranging from prey-dependent, ratio-dependent functional responses and subdiffusion. The goal of the present work is to simulate the time-dependent predator–prey model of Lotka–Volterra. Analytical solutions of this model are performed using the Laplace transform-homotopy perturbation method. The proposed scheme finds the solution without any discretization or restrictive assumptions and avoids the round-off errors. The fact that the proposed technique solves nonlinear problems without using Adomian's polynomials can be considered as a clear advantage of this algorithm over the decomposition method. We show all the possible equilibria and examine their stability in line with the ecological parameters. Numerical simulations of the diffusive predator–prey model in one-, two- and three-dimensions are given to compare and demonstrate the asymptotic behaviour of the time-dependent reaction–diffusion systems. The results show that proposed technique is a powerful tool to solve systems of nonlinear ordinary and partial differential equations of predator–prey models in ecology.

1. Introduction

The focus on fractional order differential equations has gained an increasing interest during the past few decades since they allow the understanding of the many aspects of nonlocality and spatial heterogeneity. They demonstrated various applications including continuum mechanics, viscoelastic and viscoplastic flow, and anomalous diffusion (subdiffusion, superdiffusion, non-Gaussian diffusion).[1–8] The intensive development and construction of the theory of fractional calculus played an important role in its applications in various fields of sciences such as electrical circuits, control theory, image processing, viscoelasticity, biology, and many other applications.[1,2,9–13]

The study of reaction–diffusion systems modelling spatial interactions of multi-species Lotka–Volterra models has a long standing history and has always been intriguing a lot of researchers in the fields of mathematical biology (see, for instance, Refs. 14–16). Reaction–diffusion equations are an important type of time-dependent partial differential equations that are widely used to model some of the physical, chemical, biological, and ecological processes encountered in various fields of science and engineering. They are also applied in a number of ways to model some important physical situations. For instance, the model of tissue in developmental biology via the temporal and spatial distribution of morphogen, protein trafficking within body cells, and the growth of tumors on spheres,[17] to name these only. Reaction–diffusion problems also lead to many interesting phenomena, namely, reactions and competitions in excitable media, pulse splitting and shedding processes, and stability issues.

The most important and popular type of interaction of species in the ecological study of population dynamics is predation. It describes the process between the higher species of organisms called the predator that feeds and depends solely on the lower one known as prey, for survival. The study of predator–prey models has a long-standing history dated to the pioneering work of Lotka[18] and Volterra[19,20] and since received a lot of attention since the early days of ecological science.[21–26] Since then, a lot of research work has been devoted to the study of predator–prey interactions[27–30] whose formulations were based on the Lotka–Volterra model. In the present paper, consideration is given only to a balanced fractional time reaction–diffusion system of the Lotka–Volterra type of the form

$$D_t^{\alpha} u_i(x,t) = K_i \nabla u_i + f_i(u_1, u_2, \dots, u_n), \quad i = 1, 2, \dots, n, \quad t > 0 \tag{1.1}$$

* Corresponding author.
E-mail address: kmowolabi@futa.edu.ng (K.M. Owolabi).

https://doi.org/10.1016/j.padiff.2023.100607
Received 26 October 2022; Received in revised form 29 September 2023; Accepted 11 December 2023
Available online 12 December 2023
2666-8181/© 2023 The Author(s). Published by Elsevier B.V. This is an open access article under the CC BY-NC-ND license (http://creativecommons.org/licenses/by-nc-nd/4.0/).

where α is a parameter describing the order of the fractional time derivative u_i and K_i are the population densities and diffusivities of the ith species and n being a subtle issue, is the total number of species of interacting individuals, f is the nonlinear term that accounts for the reaction part, ∇ is the Laplacian operator.

In general, there exists no method that yields an exact solution for a fractional differential equation. Therefore analytical approximations and numerical solutions are used extensively.[31,32] These include Adomain decomposition method,[33] homotopy perturbation method,[34,35] homotopy analysis method,[36,37] variational iteration method,[38] Chebyshev spectral method,[39,40] and new iterative method.[31] Among them, the new iterative method provides an effective procedure for explicit and numerical solutions of a wide and general class of differential systems representing real physical problems. The interest of the present paper lies in combining the new iterative method[31] and the Laplace transform homotopy method[41] to solve partial differential equations of time-fractional order without going through the task of computing Adomian's polynomials. The evolution of different spatiotemporal patterns arising from the coupled time-fractional reaction–diffusion system of the predator–prey model is of great importance to this study.

There are several definitions of a fractional derivative of order $\alpha > 0$ e.g Riemann–Liouville and Caputo fractional derivative. Here, some basic definitions and properties of the fractional calculus theory which can be used in this paper are presented.

The Riemann–Liouville fractional differential operator with order α is defined as

$$D^{\alpha}u(t) := \begin{cases} \frac{1}{\Gamma(n-\alpha)}\frac{d^n}{dt^n}\int_a^t \frac{u(\tau)}{(t-\tau)^{\alpha+1-n}}d\tau; & (n-1<\alpha<n\in\mathbb{N}), \\ \frac{d^n}{dt^n}u(t); & (\alpha=n\in\mathbb{N}), \end{cases} \tag{1.2}$$

where $\alpha > 0$, $t > a$ is commonly applied with the case $a = 0$, see Ref. 7 for detals.

Suppose that $\alpha > 0, t > a, \alpha, a, t \in \mathbb{R}$ Then, the fractional operator

$$D_*^{\alpha}u(t) := \begin{cases} \frac{1}{\Gamma(n-\alpha)}\int_a^t \frac{u^{(n)}(\tau)}{(t-\tau)^{\alpha+1-n}}d\tau; & (n-1<\alpha<n\in\mathbb{N}), \\ \frac{d^n}{dt^n}u(t); & (\alpha=n\in\mathbb{N}), \end{cases} \tag{1.3}$$

is referred to as the Caputo fractional derivative of order α.

In accordance with the work of Podlubny,[7] Samko et al.,[8] we present the following established properties for the Caputo fractional derivative.

Assume $n-1<\alpha<n$, for $n, m \in \mathbb{N}, \alpha \in \mathbb{R}, \lambda \in \mathbb{C}$ and $u(t), v(t)$ be such that both operators $D_*^u(t)$ and $D_*^v(t)$ exist. Then

i

$$D_*^u(t) = J^{n-\alpha}D^n u(t),$$

where

$$J^{\alpha}u(t) := \frac{1}{\Gamma(\alpha)}\int_a^t u(\tau)(t-\tau)^{\alpha-1}d\tau$$

is the known Riemann–Liouville fractional integral of order α

ii

$$\lim_{\alpha\to n} D_*^{\alpha}u(t) = u^{(n)}(t)$$
$$\lim_{\alpha\to n-1} D_*^{\alpha}u(t) = u^{(n-1)}(t) - u^{(n-1)}(0).$$

iii

$$D_*^{\alpha}(\lambda u(t) + v(t)) = \lambda D_*^{\alpha}u(t) + D_*^{\alpha}v(t).$$

iv

$$D_*^{\alpha}D^m u(t) = D_*^{\alpha+m}u(t) \neq D^m D_*^{\alpha}u(t).$$

Theorem 1.1. *Assume $t > 0$, $\alpha \in \mathbb{R}, n-1<\alpha<n\in\mathbb{N}$. the following relation between the Caputo and Riemann–Liouville fractional derivatives holds*[7]

$$D_*^{\alpha}u(t) = D^{\alpha}u(t) - \sum_{s=0}^{n-1}\frac{t^{s-\alpha}}{\Gamma(s+1-\alpha)}u^{(s)}(0).$$

Theorem 1.2.

$$D_*^{\alpha}(u(t)v(t)) = \sum_{s=0}^{\infty}\binom{\alpha}{s}\left(D^{\alpha-s}u(t)\right)v^{(s)}(t) - \sum_{s=0}^{n-1}\frac{t^{s-\alpha}}{\Gamma(s+1-\alpha)}\left[(u(t)v(t))^{(s)}(0)\right].$$

For details proof of the above theorems, readers are referred to Ref. 7.

In the present work, the Caputo time-fractional derivative operator of order $\alpha > 0$ is defined as:

$$D_t^{\alpha}u(x,t) - \begin{cases} \frac{1}{\Gamma(m-\alpha)}\int_a^t \frac{1}{(t-\xi)^{\alpha+1-m}}\frac{\partial^m u(x,\xi)}{\partial\xi^m}d\xi; & m-1<\alpha<m, m\in N, \\ \frac{\partial^m u(x,\xi)}{\partial\xi^m}; & \alpha=m\in N. \end{cases} \tag{1.4}$$

For establishing our results, we also necessarily introduce the following Riemann–Liouville fractional integral operator.

The paper is structured into 5 sections. We introduce and construct the Laplace transform homotopy perturbation method (LHPM) method in line with the functional equation in Section 2. The goal in Section 3 is to discuss the mathematical analysis of the main equation in the ecological context, and establish the conditions for the diffusive system to be Turing unstable, here two examples were considered. Some numerical experiments and results are presented in Section 4. Final conclusions are drawn in the last section.

2. Laplace transform homotopy method

The standard homotopy perturbation method (HPM) was proposed by Ji Huan He as a powerful tool to approach various kinds of nonlinear problems. The homotopy perturbation method is a combination of the classical perturbation technique and the homotopy technique (whose origin is in the topology), but not restricted to small parameters as occur with traditional perturbation methods. For example, HPM method requires neither small parameter nor linearization, but only few iterations to obtain highly accurate solutions.[32] Recently, Kamdem[42] proposed a generalized integral transform based homotopy perturbation method where various integral transforms were used. In this paper we consider the application of Laplace transform on HPM. We first define Laplace transform, inverse Laplace transform and then introduce their useful properties employed in this paper.

Definition 2.1. Laplace transform of $F(t)$ is denoted by $\mathcal{L}\{F(t)\}$ and is defined by the integral

$$\mathcal{L}\{F(t)\} = f(s) = \int_0^{\infty} e^{-st}F(t)dt. \tag{2.5}$$

The inverse is evaluated on a contour Γ, known as the Bromwich contour, as

$$\mathcal{L}^{-1}\{f(s)\} = F(t) = \int_0^{\infty} e^{st}f(s)ds. \tag{2.6}$$

The contour Γ is chosen such that it encloses all the singularities of $f(s)$.

Some known properties of LT, used in this paper are:

$$\mathcal{L}\{c_1F_1(t) + c_2F_2(t)\} = c_1f_1(s) + c_2f_2(s) \tag{2.7}$$

where c_1 and c_2 are constants and $\mathcal{L}\{F1(t)\} = f_1(s)$, $\mathcal{L}F_2(t) = f_2(s)$.

$$\mathcal{L}\{1\} = \frac{1}{s}\ (s>0), \tag{2.8}$$

$$\mathcal{L}\{t^n\} = \frac{n!}{s^{n+1}}\ (s>0), \tag{2.9}$$

$$\mathcal{L}\{F^{(n)}(t)\} = s^n f(s) - s^{n-1}F(0) - s^{n-2}F'(0) - \cdots - F^{(n-1)}(0) \tag{2.10}$$

where $F^{(n)}(t)$ denotes the nth derivatives of $F(t)$ and $\mathcal{L}\{F(t)\} = f(s)$.

Now consider the general evolutionary system of PDEs

$$D_t u(x,t) + Lu(x,t) + Nu(x,t) = g(x,t),\ t > 0 \tag{2.11}$$

with initial conditions of the form

$$u(x,0) = f(x), \tag{2.12}$$

where $x \in \mathbb{R}^n$, $u = (u_1, u_2, \dots, u_n)^T$ is the population density, with u_i the solution of the ith equation, the fist derivative time operator, L is the linear differential operator, $N = (N_1, N_2, \dots, N_n)^T$ represents the general nonlinear differential operator and $g(x,t)$ is the source term.

In order to solve the system of PDEs (2.11) by the means of homotopy method, we first apply the Laplace transform on both side of Eq. (2.11), we have

$$\mathcal{L}\left\{D_t u(x,t) + Lu(x,t) + Nu(x,t)\right\} = \mathcal{L}\{g(x,t)\}. \tag{2.13}$$

Using the differentiation property of the Laplace transform and above initial conditions, after algebraic simplifications we have

$$\mathcal{L}\left\{u(x,t)\right\} = \frac{u(x,0)}{s} + \frac{\mathcal{L}\{g(x,t)\}}{s^\alpha} - \frac{1}{s^\alpha}\left(\mathcal{L}\left\{Lu(x,t) + Nu(x,t)\right\}\right). \tag{2.14}$$

Now applying the inverse Laplace transform on both sides of Eq. (2.14), we obtain

$$u(x,t) = G(x,t) - \mathcal{L}^{-1}\left\{\frac{1}{s^\alpha}\left(\mathcal{L}\left\{Lu(x,t) + Nu(x,t)\right\}\right)\right\}, \tag{2.15}$$

where $G(x,t)$ represents the term arising from the source term and the prescribed initial conditions.

We then construct the following homotopy

$$u(x,t) = G(x,t) - p\left(\mathcal{L}^{-1}\left\{\frac{1}{s^\alpha}\left(\mathcal{L}\left\{Lu(x,t) + Nu(x,t)\right\}\right)\right\}\right), \tag{2.16}$$

According to standard homotopy perturbation method the solution u can be expanded into infinite series as

$$u(x,t) = \sum_{j=0}^{\infty} p^j u_j(x,t), \tag{2.17}$$

where $p \in [0,1]$ is an embedding parameter and $u_j,\ j = 0, 1, \dots$ are unknown functions to be determined. The nonlinear operator N is expanded as Ref. 31

$$\begin{aligned} N\left(\sum_{j=0}^{\infty} p^j u_j\right) &= p^0 N(u_0) + p^1\left\{N(u_0+u_1) - N(u_0)\right\} \\ &\quad + p^2\left\{N(u_0+u_1+u_2) - N(u_0+u_1)\right\} \\ &\quad + p^3\left\{N(u_0+u_1+u_2+u_3) - N(u_0+u_1+u_2)\right\} + \cdots \\ &= N\left(u_0\right) + \sum_{j=1}^{\infty} p^j\left\{N\left(\sum_{i=0}^{j} u_i\right) - N\left(\sum_{i=0}^{j-1} u_i\right)\right\} \\ &= N\left(u_0\right) + \sum_{j=1}^{\infty} p^j H_j(u), \end{aligned} \tag{2.18}$$

where

$$H_j(u_0, u_1, \dots, u_n) = N\left(\sum_{j=0}^{n} u_j\right) - N\left(\sum_{j=0}^{n-1} u_j\right),\ n = 0, 1, 2, 3 \dots. \tag{2.19}$$

We substitute (2.17) and (2.18) into (2.20) yields

$$\sum_{n=0}^{\infty} p^n u_n(x,t) = G(x,t) - \mathcal{L}^{-1}\left\{\frac{1}{s^\alpha}\left(\mathcal{L}\left\{L\sum_{j=0}^{\infty} p^j u_j(x,t) + \sum_{j=0}^{\infty} p^j H_j(u)\right\}\right)\right\}, \tag{2.20}$$

and equate the coefficients of p with the same powers to obtain

$$\begin{aligned} p^0 &: u_0(x,t) = G(x,t), \\ p^1 &: u_1(x,t) = -\mathcal{L}^{-1}\left\{\frac{1}{s^\alpha}\left(\mathcal{L}\left\{Lu_0(x,t) + H\left(u_0\right)\right\}\right)\right\} \\ p^2 &: u_2(x,t) = -\mathcal{L}^{-1}\left\{\frac{1}{s^\alpha}\left(\mathcal{L}\left\{Lu_1(x,t) + H\left(u_0, u_1\right)\right\}\right)\right\} \\ &\vdots \\ p^n &: u_n(x,t) = -\mathcal{L}^{-1}\left\{\frac{1}{s^\alpha}\left(\mathcal{L}\left\{Lu_{n-1}(x,t) + H\left(u_0, u_1, \dots, u_{n-1}\right)\right\}\right)\right\} \\ &\vdots \end{aligned} \tag{2.21}$$

The utility of HPM is tested on practical problems that model diffusive predator–prey in ecology.

2.1. The Caputo fractional derivative

The Riemann–Liouville fractional integration of order α is given as

$$\begin{aligned} J^\alpha f(x) &= \frac{1}{\Gamma(\alpha)}\int_0^x (x-t)^{\alpha-1} f(t)dt,\quad \alpha > 0,\quad x > 0, \\ J^0 f(x) &= f(x). \end{aligned}$$

As another property, operator J^α can be given as

$$J^\alpha x^\beta = \frac{\Gamma(\beta+1)}{\Gamma(\alpha+\beta+1)} x^{\alpha+\beta}.$$

We can now define the Caputo fractional derivative of order α as

$$D^\alpha f(x) = J^{m-\alpha}\left(\frac{d^m}{dx^m} f(x)\right),$$

where $m - 1 < \alpha \le m,\ m \in N,\ m > \alpha,\ m$ defines the smallest integer.[43]

The Caputo's fractional differentiation is expressed as a linear operation

$$D^\alpha(\lambda f(x) + \omega g(x)) = \lambda D^\alpha f(x) + \omega D^\alpha g(x), \tag{2.22}$$

where λ and ω are constants. In Caputo sense, we have

$$D^\alpha a = 0,\ (a \text{ is a constant}) \tag{2.23}$$

$$D^\alpha x^\beta = \begin{cases} 0, & \text{for } \beta \in N_0 \text{ and } \beta < \lceil\alpha\rceil \\ \frac{\Gamma(\beta+1)}{\Gamma(\alpha+\beta+1)} x^{\beta-\alpha}, & \text{for } \beta \in N_0 \text{ and } \beta \ge \lceil\alpha\rceil \text{ or } \beta \ni N \text{ and } \beta > \lfloor\alpha\rfloor. \end{cases} \tag{2.24}$$

The ceiling and floor functions are used to represent the smallest integer greater than or equal to α and largest integer less than or equal to α respectively. For $N = \{1, 2, \dots\}$ and $N_0 = \{0, 1, 2, \dots\}$.

2.2. Chebyshev polynomials

The Chebyshev polynomials defined on the interval $(-l, l)$ can be determined by using the recurrence equation

$$T_{i+l} = 2tT_i(t) - T_{i-l}(t),\quad i = 1, 2, \dots,$$

where $T_0(t) = l$ and $T_l(t) = t$. We let $l = 1$ for simplicity. In attempt to use the polynomials on the spatial interval $x \in (0, L)$, we define the well-known shifted Chebyshev polynomials by using a change of variable $t = \frac{2x}{L} - 1$. If the shifted Chebyshev polynomials $T_i(\frac{2x}{L} - 1)$ is represented by $T_{L,i}(x)$, then we can generate $T_{L,i}(x)$ by the recurrence relation

$$T_{L,i+1}(x) = 2\left(\frac{2x}{L} - 1\right)T_{L,i}(x) - T_{L,i-1}(x),\quad i = 1, 2, \dots,$$

where $T_{L,0}(x) = 1$ and $T_{L,1}(x) = \frac{2x}{L} - 1$, whose analytical form is given by

$$T_{L,1}(x) = i\sum_{k=0}^{i}(-1)^{i-k}\frac{(i+k-1)!2^{2k}}{(i-k)!(2k)!L^k}x^k, \tag{2.25}$$

where $T_{L,j}(0) = (-1)^i$ and $T_{L,i}(L) = 1$. The orthogonality condition is expressed in the form

$$\int_0^L T_{L,j}(x)T_{L,k}(x)H_L(x)dx = \delta_{jk}h_k,$$

where $H_L(x) = \frac{1}{\sqrt{L_x - x^2}}$ and $h_k = \frac{a_k}{2}\pi$ with $a_0 = 2,\ a_i = 1,\ 1 \geq 1$.

In other words, any function $u(x)$, that is square integrable in interval $(0, L)$ can be defined in terms of shifted Chebyshev polynomials as

$$u(x) = \sum_{j=0}^{\infty} c_j T_{L,j}(x),$$

where c_j are the given coefficients defined by

$$c_j = \frac{1}{h_j}\int_0^L u(x)T_{L,j}(x)H_L(x)dx, \quad j = 0, 1, 2, \ldots \tag{2.26}$$

Clearly, it is only the first $(N + 1)$ terms of the shifted Chebyshev polynomials that are considered in practice. Hence we let

$$u_N(x) \simeq \sum_{j=0}^{N} c_j T_{L,j}(x).$$

By turning to the Chebyshev–Gauss interpolation. We indicate by $x_{N,j},\ 0 \leq j \leq N$, the nodes of the standard Chebyshev–Gauss interpolation on the interval $(-l, l)$ for $l = 1$. We give the corresponding Christoffel numbers by $G_{N,j},\ 0 \leq j \leq N$, the nodes of the shifted Chebyshev–Gauss interpolation on the interval $(0, L)$ is given as the zeros of $T_{L,N+1}(x)$ denoted by $x_{L,N,j}\ 0 \leq j \leq N$. It follows that for any $\psi \in P_{2N+1}(0, L)$, we have

$$\begin{aligned}\int_0^L H_L(x)\psi(x)dx &= \int_{-1}^{1} \frac{1}{\sqrt{1-x^2}}\psi\left(\frac{L}{2}(x+1)\right)dx \\ &= \sum_{j=0}^{N} G_{N,j}\psi\left(\frac{1}{2}(x_{N,j}+1)\right) \\ &= \sum_{j=0}^{N} G_{L,N,j}\psi(x_{L,N,j}).\end{aligned}$$

2.3. Fractional derivatives of $T_{L,i}(x)$

The aim of this section is give prove to proposed theorem on the fractional derivatives of the shifted Chebyshev polynomials.

Proposition 2.2. *Let $T_{L,i}(x)$ be a shifted Chebyshev polynomial, then*

$$D^\alpha T_{L,i}(x) = 0, \quad i = 0, 1, 2, \ldots, \lceil\alpha\rceil - 1, \quad \alpha > 0.$$

Proof. The proof follows directly from the relations in (2.22)–(2.24) with (2.25). □

Theorem 2.3. *In the Caputo sense, the fractional derivative of order α for the Chebyshev polynomials is given by*

$$D^\alpha T_{L,i}(x) = \sum_{j=0}^{\infty} P_\alpha(i,j)T_{L,j}(x), \quad i = \lceil\alpha\rceil, \lceil\alpha\rceil + 1, \ldots,$$

where

$$P_\alpha(i,j) = \sum_{k=\lceil\alpha\rceil}^{i} \frac{(-1)^{i-k}2i(i+k-1)!\Gamma(k-\alpha+\frac{1}{2})}{a_j L^\alpha \Gamma(k+\frac{1}{2})!(i-k)!\Gamma(k-\alpha-j+1)\Gamma(k+j-\alpha+1)}.$$

Proof. The analytical form of the shifted Chebyshev polynomials $T_{L,i}(x)$ of degree i is expressed by (2.25). By using Eqs. (2.23)–(2.25) we obtain

$$\begin{aligned}D^\alpha T_{L,i}(x) &= i\sum_{k=0}^{i}(-1)^{i-k}\frac{(i+k-1)!2^{2k}}{(i-k)!(2k)!L^k}D^\alpha x^k \\ &= i\sum_{k=\lceil\alpha\rceil}^{i}(-1)^{i-k}\frac{(i+k-1)!2^{2k}k!}{(i-k)!(2k)!L^k\Gamma(k-\alpha+1)}x^{k-\alpha}, \\ &\quad i = \lceil\alpha\rceil, \lceil\alpha\rceil+1, \ldots\end{aligned} \tag{2.27}$$

Now, we can express the term $x^{k-\alpha}$ in the form of shifted Chebyshev series, so that we get

$$x^{k-\alpha} = \sum_{j=0}^{\infty} b_{bk}T_{L,j}(x), \tag{2.28}$$

where b_{kj} is defined in (2.26) with $u(x) = x^{k-\alpha}$, and

$$b_{kj} = \begin{cases} \frac{1}{\sqrt{\pi}}\frac{L^{k-\alpha}\Gamma(k-\alpha+1/2)}{\Gamma(k-\alpha+1)}, & j=0 \\ \frac{jL^{k-\alpha}}{\sqrt{\pi}}\sum_{r=0}^{j}(-1)^{j-r}\frac{(j+r-1)!2^{2r+1}\Gamma(k+r-\alpha+1/2)}{(j-r)!(2r)!\Gamma(k+r-\alpha)}, & j=1,2,\ldots \end{cases} \tag{2.29}$$

By using Eqs. (2.27)–(2.29), we have

$$D^\alpha T_{L,i}(x) = \sum_{j=0}^{\infty} P_\alpha(i,j)T_{L,j}(x), \quad i = \lceil\alpha\rceil, \lceil\alpha\rceil+1, \ldots,$$

where $P_\alpha(i,j) = \sum_{k=\lceil\alpha\rceil}^{i}\vartheta_{ijk}$, and

$$\vartheta_{ijk} = \begin{cases} \frac{i(-1)^{i-k}(i+k-1)!2^{2k}k!\Gamma(k-\alpha+1/2)}{L^\alpha(i-k)!(2k)!\sqrt{\pi}((k-\alpha+1))^2}, & j=0, \\ \frac{(-1)^{i-k}ij(i+k-1)!2^{2k+1}k!}{L^\alpha(i-k)!(2k)!\sqrt{\pi}(k-\alpha+1)}\times\sum_{r=0}^{j}\frac{(-1)^{j-r}(j+r-1)!2^{2r}\Gamma(k+r-\alpha+1/2)}{(j-r)!(2r)!\Gamma(k+r-\alpha+1)}, & j=1,2,\ldots \end{cases} \tag{2.30}$$

After some algebraic manipulations, we write $\vartheta_{i,j,k}$ in the form

$$\vartheta_{ijk} = \frac{(-1)^{i-k}2i(i+k-1)!\Gamma(k-\alpha+\frac{1}{2})}{a_j L^\alpha\Gamma(k+\frac{1}{2})(i-k)!\Gamma(k-\alpha-j+1)\Gamma(k+j-\alpha+1)}, \quad j = 0, 1, \ldots \tag{2.31}$$

The proof is completed by Eq. (2.31) which gives the desired result. □

3. Mathematical analysis of the main equation

We begin our analysis by considering in just one-dimensional space the time-fractional reaction–diffusion equation

$$\left.\begin{aligned}\frac{\partial^\alpha u(x,t)}{\partial t^\alpha} &= D_u\nabla^2 u(x,t) + \mathcal{F}(u,v), \\ \frac{\partial^\alpha v(x,t)}{\partial t^\alpha} &= D_v\nabla^2 v(x,t) + \mathcal{G}(u,v),\end{aligned}\right\} \tag{3.32}$$

with certain initial conditions on the intervals $[-L, L]$ or $[0, L]$ subject to the Neumann boundary conditions

$$\left.\frac{\partial u}{\partial x}\right|_{x=0} = \left.\frac{\partial u}{\partial x}\right|_{x=L} = 0,$$

where $\frac{\partial^\alpha u(x,t)}{\partial t^\alpha}$ represents the Caputo time-fractional derivative of order $0 < \alpha < 2$ defined as Refs. 2, 44

$$\frac{\partial^\alpha}{\partial t^\alpha}u(t) := \frac{1}{\Gamma(s-\alpha)}\int_0^t \frac{u^{(s)}(\tau)}{(t-\tau)^{\alpha+1-s}}d\tau, \quad s-1 < \alpha < s,\ s \in N,$$

with similar expression for v. $\nabla^2 = \frac{\partial^2}{\partial x^2}$, $u(x,t),\ v(x,t) \in \mathbb{R}$, $x, t \in \mathbb{R}$ and $\mathcal{F}, \mathcal{G} \in \mathbb{R}$ are the nonlinear functions of the equation modelling their rate of productions, $D_u, D_v \in \mathbb{R}$ are positive diffusivity constants.

At $\alpha = 1$, Eq. (3.32) corresponds to classical time-dependent reaction–diffusion system. At $\alpha < 1$ and $\alpha > 1$, it describes anomalous subdiffusive and superdiffusive scenarios respectively.

3.1. Linear stability analysis

In this segment, we follow the stability idea as widely reported for some parabolic models of predator–prey type.[45–50] By linearization, we can analyse the stability of the steady state solutions of (3.32) which corresponds to the homogeneous equilibrium states

$$\mathcal{F}(u,v) = 0, \quad \mathcal{G}(u,v) = 0. \tag{3.33}$$

We transform (3.32) to linear system

$$\frac{\partial^\alpha \mathbf{u}(x,t)}{\partial t^\alpha} = \mathbf{A}\mathbf{u}(x,t), \tag{3.34}$$

where

$$\mathbf{A} = \begin{bmatrix} D_u\nabla^2 - a_{11} & -a_{12} \\ -a_{21} & D_v\nabla^2 - a_{22} \end{bmatrix}, \quad \mathbf{u}(x,t) = \begin{bmatrix} \Delta u(x,t) \\ \Delta v(x,t) \end{bmatrix}$$

and $a_{11} = \mathcal{F}'u$, $a_{12} = \mathcal{F}'v$, $a_{21} = \mathcal{G}'u$, $a_{22} = \mathcal{G}'v$. The derivatives are taken to satisfy condition in (3.33). By putting the solution of the form

$$\mathbf{u}(x,t) = \begin{bmatrix} \Delta u(t) \\ \Delta v(t) \end{bmatrix} \cos kx, \; k = \frac{\pi}{L} j, \; j = 1, 2, \ldots$$

into the fractional reaction–diffusion system (3.32), we obtain the system of ordinary differential equations (ODEs) (3.34).

By seeking for the solution of the linear equation in the form

$$\mathbf{u}(x,t) = \begin{bmatrix} \Delta u(t) \\ \Delta v(t) \end{bmatrix} \exp(\lambda t) \cos kx,$$

we obtain a homogeneous system of linear equations for $\Delta u, \Delta v$, which on solving results the characteristic equation

$$\det |\lambda \mathbf{I} - \mathbf{A}| = 0, \tag{3.35}$$

where $\mathbf{I}$ is the identity matrix, and

$$\mathbf{A} = -\begin{bmatrix} D_u\nabla^2 + a_{11} & a_{12} \\ a_{21} & D_v\nabla^2 + a_{22} \end{bmatrix}. \tag{3.36}$$

For the diffusive case at $\alpha = 1$, the boundary value problem for system (3.32) is known to be unstable (Turing Bifurcation) in accordance with inhomogeneous wave vectors $k \neq 0$ if $tr\mathbf{A} < 0$ and $\det \mathbf{A} < 0$, that is

$$a_{11} < -\left[(D_u/D_v)^2 a_{22} + 2(D_u/D_v)(a_{22}a_{11} - a_{12}a_{21})^{1/2}\right]$$

$$(a_{11} + k^2 D_u^2) + (a_{22} + k^2 D_v^2) > 0, \; a_{22}a_{11} - a_{12}a_{21} > 0$$

and (Hopf Bifurcation) in accordance with the homogeneous ($k = 0$) instabilities, if $tr\mathbf{A} > 0$ and $\det \mathbf{A} > 0$, that is

$$a_{11} + a_{22} < 0, \; a_{22}a_{11} - a_{12}a_{21} > 0.$$

Generally speaking, for the elements a_{ij} of the community matrix for a multi-stable system such as (3.32), the inequalities $a_{11} > 0, a_{12} < 0, a_{21} > 0, a_{22} < 0$ are satisfied in the case of an unstable steady-state solution while the inequalities $a_{11} < 0, a_{12} < 0, a_{21} > 0, a_{22} < 0$ must hold true for a stable steady-state solution. For homogeneous perturbations ($k = 0$) we have in this scenario $\det \mathbf{A}(0) = a_{11}a_{22} - a_{12}a_{21} < 0$ for an unstable state, and $\det \mathbf{A}(0) > 0$ for the stable case.

Linear transformation of (3.34) at the neighbourhood of homogeneous state yield a diagonal form

$$\frac{d^\alpha \omega(t)}{dt^\alpha} = \mathcal{A}\omega(t), \tag{3.37}$$

where $\mathcal{A}$ denotes a diagonal matrix of $\mathbf{A}$,

$$\mathcal{A} = \mathbf{B}^{-1}\mathbf{A}\mathbf{B} \begin{bmatrix} \lambda_1 & 0 \\ 0 & \lambda_2 \end{bmatrix}.$$

The values of λ_1 and λ_2 are determined from the characteristic equation $\lambda^2 - tr\mathbf{A} + \det \mathbf{A} = 0$ in conjunction with matrix (3.36) as

$$\lambda_{1,2} = \frac{tr\mathbf{A} \pm \sqrt{tr^2\mathbf{A} - 4\det \mathbf{A}}}{2}, \quad \omega(t) = \mathbf{B}^{-1} \begin{bmatrix} \Delta u(t) \\ \Delta v(t) \end{bmatrix},$$

where $\mathbf{B}$ denotes the matrix eigenvectors of $\mathbf{A}$.

Following the Mittag-Leffler functions as reported by Refs. 51, 52, we report the solution of (3.37) as

$$\Delta u(t) = \sum_{k=0}^{\infty} \frac{(\lambda_1 t^\alpha)^k}{\Gamma(k\alpha + 1)} \Delta u(0) = Q_\alpha(\lambda_1 t^\alpha)\Delta u(0),$$

$$\Delta v(t) = \sum_{k=0}^{\infty} \frac{(\lambda_2 t^\alpha)^k}{\Gamma(k\alpha + 1)} \Delta v(0) = Q_\alpha(\lambda_2 t^\alpha)\Delta v(0).$$

If for any of the roots $|\arg(\lambda_i)| < \alpha\pi/2, \; i = 1, 2$, the solution possess an increasing function component, then we can deduce that the system is asymptotically unstable. By analysing the roots (3.35), obviously $4\det \mathbf{A} - tr^2\mathbf{A} > 0$ which has the representation

$$\lambda_{1,2} = \frac{tr\mathbf{A} \pm i\sqrt{-tr^2\mathbf{A} + 4\det \mathbf{A}}}{2} \equiv \underbrace{\lambda}_{Re} \pm \underbrace{i\lambda}_{Im}.$$

The marginal value $\alpha : a_0 = \frac{2}{\pi}|\arg(\lambda_i)|$ which follows from $|\arg(\lambda_i)| < \alpha\pi/2$ is denoted by the formula

$$\left.\begin{array}{ll} \frac{2}{\pi}\arctan\sqrt{4\det \mathbf{A}/tr^2\mathbf{A} - 1}, & tr\mathbf{A} \geq 0, \\ 2 - \frac{2}{\pi}\arctan\sqrt{4\det \mathbf{A}/tr^2\mathbf{A} - 1}, & tr\mathbf{A} \leq 0 \end{array}\right\} = a_0. \tag{3.38}$$

The derivative order a_0 for systems (3.32) is seen as an additional bifurcation parameter that changes the stability of homogeneous stationary solutions. For instance, at $\alpha = 1$, the domain is unstable if $tr\mathbf{A} < 0$ and stable if otherwise. At lower $\alpha : \alpha < a_0 = \frac{2}{\pi}|\arg(\lambda_i)|$, that is, $\alpha \in [0, a_0]$ the system is stable but has some oscillatory modes. As the value of α is increased and larger than a_0, $\alpha > a_0 = \frac{2}{\pi}|\arg(\lambda_i)|$ the system results to oscillatory instability.

3.2. The modified Lotka–Volterra predator–prey system

To start with, we consider the modified Lotka–Volterra system for the waves of pursuit and evasion in the predator–prey system of equations[53]

$$\begin{aligned} \frac{\partial^\alpha u}{\partial t^\alpha} - D_u\nabla u &= \mathcal{F}(u,v) = au\left(1 - \frac{u}{\kappa}\right) - buv \\ \frac{\partial^\alpha v}{\partial t^\alpha} - D_v\nabla v &= \mathcal{G}(u,v) = cuv - dv \end{aligned} \tag{3.39}$$

with logistic growth of the prey, where u and v are the population densities of the prey and predator species respectively, κ is the carrying capacity of the prey, constants a, b, c and d are positive parameters, while D_u and D_v are the diffusion coefficients, the Laplacian operator $\nabla u = \partial^2 u/\partial x^2$ (henceforth) in one dimensional space. Following the ideas in Refs. 54, 55, the number of parameters in (3.39) can be reduced by choosing

$$\tilde{t} = at, \tilde{u} = \frac{u}{\kappa}, \tilde{v} = \frac{bv}{a}, \tilde{x} = x\sqrt{\frac{a}{D_v}}, \tilde{D} = \frac{D_u}{D_v}, \gamma = \frac{c\kappa}{a}, \beta = dc\kappa, \tag{3.40}$$

the tildes are neglected to arrive at the following system with dimensionless quantities:

$$\begin{aligned} \frac{\partial^\alpha u}{\partial t^\alpha} &= D\frac{\partial^2 u}{\partial x^2} + u(1 - u - v) \\ \frac{\partial^\alpha v}{\partial t^\alpha} &= \frac{\partial^2 v}{\partial x^2} + \gamma v(u - \beta). \end{aligned} \tag{3.41}$$

Populations distribution and phase portraits of the non-diffusive form of models (3.39) and (3.41) are respectively given in Figs. 1 and 2 for different instances of α. The similarity in results obtained for these two models at $\alpha = 0.97$ shows that the dimensional parameters introduced in (3.40) above is correct. The system (3.41) has three stationary points in the absence of diffusion. That is, point $(\hat{u}, \hat{v}) = (0, 0)$ corresponds to the extinction of both prey and predator, point $(\hat{u}, \hat{v}) = (1, 0)$ corresponds to the existence of only the prey species and the third point $(\hat{u}, \hat{v}) = (\beta, 1 - \beta)$ shows the coexistence of both species provided $\beta < 1$.

To obtain the travelling wave solution, we introduce a new variable $\xi = x + ct$, so that $u(x,t) = \phi(\xi)$ and $v(x,t) = \varphi(\xi)$. By assuming $D = 0$, the number of ODE system reduced from four to three equations

$$\begin{aligned} \phi' &= \frac{\phi - \phi^2 - \phi\varphi}{c} \\ \varphi' &= \psi \\ \psi' &= c\psi - \gamma\varphi(\phi - \beta), \end{aligned} \tag{3.42}$$

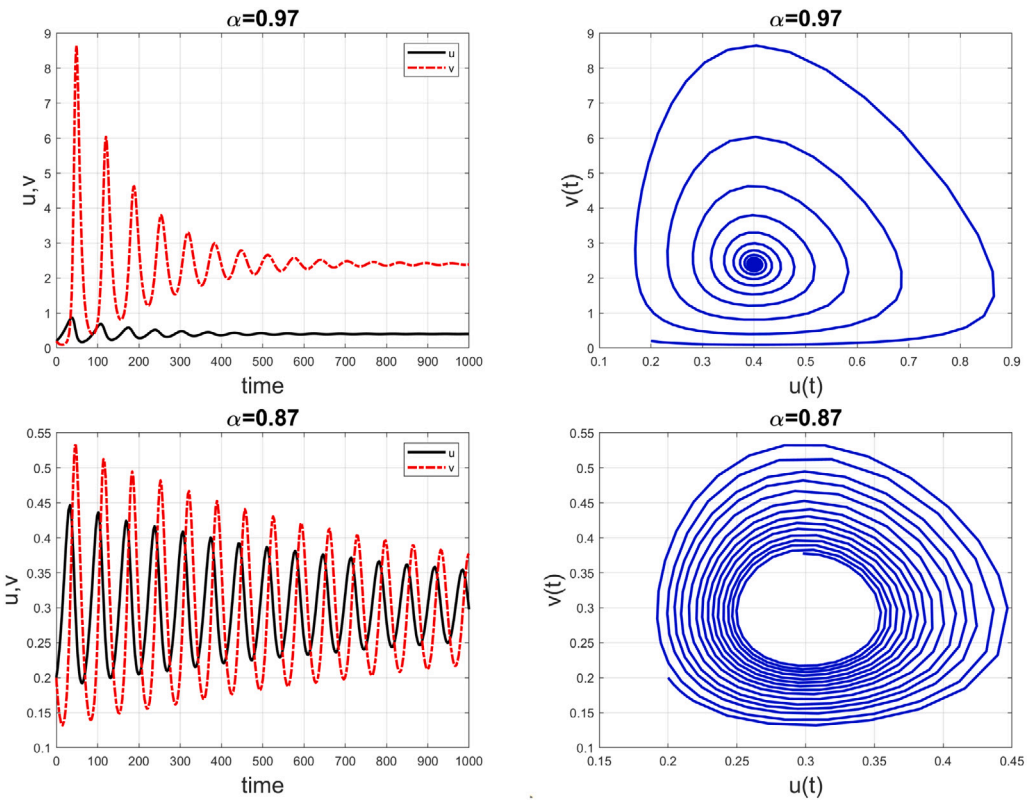

Fig. 1. (a) Dynamic behaviour of non-diffusive form of (3.39) showing the phase portraits and time-series solutions for the prey–predator species at different instances fractional order α, with parameters $a = 0.06, \kappa = 0.5, b = 0.02$ and $c = 0.5$.

where c is the wave speed. As a result, the three new stationary points of (3.42) are

$$(\hat{\phi}, \hat{\varphi}, \hat{\psi}) = (0,0,0), (\hat{\phi}, \hat{\varphi}, \hat{\psi}) = (1,0,0) \text{ and } (\hat{\phi}, \hat{\varphi}, \hat{\psi}) = (\beta, 1-\beta, 0).$$

The general community matrix is given as

$$\mathbf{A} = \begin{pmatrix} \frac{1-2\phi-\varphi}{c} & -\frac{\phi}{c} & 0 \\ 0 & 0 & 1 \\ -\gamma\varphi & -\gamma(\phi-\beta) & c \end{pmatrix}_{(\hat{\phi},\hat{\varphi},\hat{\psi})}.$$

Setting $|\mathbf{A} - \lambda\mathbf{I}|$ at point $(\hat{\phi}, \hat{\varphi}, \hat{\psi}) = (0,0,0)$, we have corresponding eigenvalues

$$\lambda_1 = \frac{1}{c}, \lambda_2 = \frac{c + \sqrt{c^2 + 4\gamma\beta}}{2} \text{ and } \lambda_3 = \frac{c - \sqrt{c^2 + 4\gamma\beta}}{2}.$$

For stability, we require that $Re\lambda < 0$, so the point $(0,0,0)$ is unstable.

Again, for the second point $(\hat{\phi}, \hat{\varphi}, \hat{\psi}) = (1,0,0)$, we obtain

$$\lambda_1 = -\frac{1}{c}, \lambda_2 = \frac{c + \sqrt{c - 4\gamma(1-\beta)}}{2} \text{ and } \lambda_3 = \frac{c - \sqrt{c - 4\gamma(1-\beta)}}{2},$$

we have unstable manifold for $c > 0$, λ_1, $\lambda - 2 > 0$ and oscillatory unstable for $c^2 < 4\gamma(1-\beta)$. For the possibility of the travelling wave to exist, we require that $c^2 \geq 4\gamma(1-\beta)$ for $\beta < 1$.

For the third stationary point $(\hat{\phi}, \hat{\varphi}, \hat{\psi}) = (\beta, 1-\beta, 0)$, we have the eigenvalues corresponding to the polynomial

$$\chi(\lambda) = \lambda^3 - \lambda^2\left(c - \frac{\beta}{c}\right) - \lambda\beta - \frac{\gamma\beta(1-\beta)}{c} = 0.$$

With $\gamma = 0$, we obtain the eigenvalues

$$\lambda_1 = 0,\ \lambda_2 = \frac{\left(c - \frac{\beta}{c}\right) + \sqrt{\left(c - \frac{\beta}{c}\right)^2 + 4\beta}}{2} \text{ and}$$

$$\lambda_3 = \frac{\left(c - \frac{\beta}{c}\right) - \sqrt{\left(c - \frac{\beta}{c}\right)^2 + 4\beta}}{2}.$$

It is known that the point $(\beta, 1-\beta, 0)$ has two stable and one unstable directions and the value of γ actually dictates the type of wave profiles. If $\gamma < \tilde{\gamma}$ we have two negative roots and obtain a monotonic wave, but if $\gamma > \tilde{\gamma}$ we have complex negative roots with negative real parts, the wave profiles here becomes oscillatory.

3.3. Predator–prey model with Holling type II functional response

For the second dynamical system, we are consider the time-fractional predator–prey system with a logistic growth[30,56]

$$\begin{aligned} \frac{\partial^\alpha u}{\partial t^\alpha} D_u \Delta u &= f(u,v) = u(1-u) - \frac{uv}{u+\phi} \\ \frac{\partial^\alpha v}{\partial t^\alpha} - D_v \Delta v &= g(u,v) = \psi\frac{uv}{u+\phi} - \varphi v. \end{aligned} \tag{3.43}$$

where $u(\cdot,t)$ and $u(\cdot,t)$ are the prey and predator population densities at time t and positions x, y, respectively. Parameters ϕ, ψ and φ are strictly positive, and D_u, D_v are the diffusion coefficients of both species, $f(u,v)$ and $g(u,v)$ are the reaction kinetics. The symbol Δ is the Laplacian operator defined in one and two dimensions as

$$\Delta = \frac{\partial^2}{\partial x^2} \quad \text{or} \quad \Delta = \left(\frac{\partial^2}{\partial x^2} + \frac{\partial^2}{\partial y^2}\right),$$

respectively. The predator–prey model (3.43) is subjected to initial condition

$$u(x,y,0) = u_0(x,y), \quad v(x,y,0) = v_0(x,y), \quad (x,y) \in \Omega, \tag{3.44}$$

and the Neumann (zero-flux) boundary conditions

$$\frac{\partial u}{\partial \nu} = 0, \quad \frac{\partial v}{\partial \nu} = 0, \quad (x,y) \in \partial\Omega, \quad t > 0 \tag{3.45}$$

where ν denotes the outward normal to domain boundary $\partial\Omega$. The corresponding non-spatial form predator–prey model (3.43) with $D_u = D_v = 0$ is given by

$$\frac{d^\alpha u}{dt^\alpha} = f(u,v) = u(1-u) - \frac{uv}{u+\phi}$$

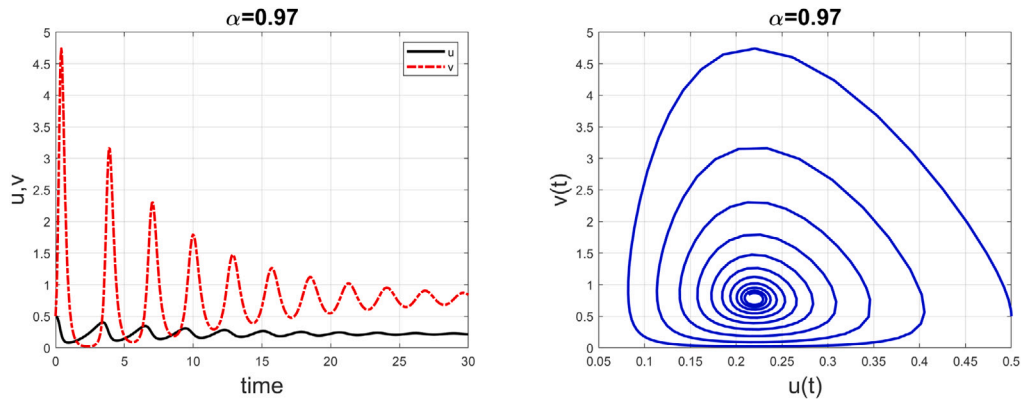

Fig. 2. (a) Dynamic behaviour of non-diffusive form of (3.41) showing the phase portraits and time-series solutions for the prey-predator species at $\alpha = 0.97$, with $\gamma = 12.5$ and $\beta = 0.2$.

$$\frac{d^\alpha v}{dt^\alpha} = g(u,v) = \psi\frac{uv}{u+\phi} - \varphi v. \tag{3.46}$$

To study the spatiotemporal dynamics of the predator–prey model, for the sake of brevity, we choose $\alpha = 1$, and consider the linear stability of model (3.46). In order to give a good guideline on the appropriate choice of parameters for numerical simulation of the full fractional reaction–diffusion model, it is mandatory to consider the local dynamics of the system.[30,57–59] So, naturally, the dynamic in the biologically feasible regions $u \geq 0, v \geq 0$ which show the existence of both prey and predator species should be of important interest.

A simple calculation shows that model (3.46) has three equilibrium states $E_0 = (0,0)$, $E_1 = (1,0)$ and $E^* = (u^*, v^*)$ which correspond to the total extinction of both prey and predator species, existence of only the prey population, and nontrivial state which guarantee that both species exist and permanent in a given habitat. The first two states are trivial and saddle, the point $E^* = (u^*, v^*)$ is calculated as

$$u^* = \frac{\phi\varphi}{\psi-\varphi}, \quad \psi > \varphi, \quad \text{and} \quad v^* = \frac{\phi\psi^2 - \psi\varphi\phi^2 - \psi\varphi\phi}{\varphi^2+\phi}, \quad \phi < \frac{\psi-\varphi}{\varphi}. \tag{3.47}$$

By linearizing the dynamic model (3.46) about the positive equilibrium point $E^* = (u^*, v^*)$ leads to the community matrix $\mathbf{B}$ defined by

$$\mathbf{B}_{E^*} = \begin{pmatrix} b_{11} & b_{12} \\ b_{21} & b_{22} \end{pmatrix} \tag{3.48}$$

where

$$b_{11} = -\frac{\phi\varphi(\varphi\phi^2\psi - \phi\psi^2 + \varphi\phi\psi)}{(\psi-\varphi)\left(\phi + \frac{\phi\varphi}{\psi-\varphi}\right)^2(\psi^2 - 2\psi\varphi + \varphi^2)} + 1,$$

$$b_{12} = \frac{\phi\varphi}{(\psi-\varphi)\left(\phi + \frac{\phi\varphi}{\psi-\varphi}\right)},$$

$$b_{21} = \frac{\phi\varphi(\varphi\phi^2\psi - \phi\psi^2 + \varphi\phi\psi)}{(\psi-\varphi)\left(\phi + \frac{\phi\varphi}{\psi-\varphi}\right)^2(\psi^2 - 2\psi\varphi + \varphi^2)},$$

$$b_{22} = \frac{\phi\psi\varphi}{(\psi-\varphi)\left(\phi + \frac{\phi\varphi}{\psi-\varphi}\right)} - \varphi.$$

The corresponding characteristic polynomial is computed as

$$\lambda^2 + \mathscr{A}\lambda + \mathscr{B} = 0, \tag{3.49}$$

where

$$\mathscr{A} = -(a_{11} + a_{22}), \quad \text{and} \quad \mathscr{B} = -a_{11}a_2 - a_{12}a_{21},$$

and the roots of (3.49) are

$$\lambda_{a,b} = \frac{1}{2}(-\mathscr{A} \pm \sqrt{\mathscr{A}^2 - 4\mathscr{B}}). \tag{3.50}$$

So, based on the value of roots λ_a and λ_b the equilibrium state E^* can be categorized as whether it is a saddle, node, spiral or centre. The nature of these roots also inform us whether the state E^* is stable or unstable. For further studies on the analysis of reaction–diffusion systems considered in this paper, we refer our reader to see the work of Refs. 54, 59–66. For spatiotemporal evolution of model (3.43), we choose $\phi = 0.3, \psi = 2, \varphi = 0.8$, and we the ratio of diffusion coefficients express as $\delta = D_v/D_u$. The local phase place and time series solution of (3.46) is given in Fig. 3.

4. Numerical simulations

In this section, we investigate the efficiency and accuracy of the proposed method when applied to solve two-variable time-fractional-reaction–diffusion system modelling the spatial interactions between the prey u, and predator v. Before going to the simulations perse, we need to remind ourselves that we are mainly interested in the coexistence of the steady state. For instance, the dynamic system (3.39) consists of three spatially uniform steady state solutions $(\hat{u}, \hat{v}) = (0,0), (1,0)$ and $(\beta, 1-\beta)$. We consider the latter to be nontrivial and biologically meaningful only if the $0 < \beta < 1$ which in the present case represents the coexistence of the species. So, on this note we are thus involved in simulating frameworks on which we can hang our understanding. Also, it worth mentioning that whenever the condition $0 < \beta < 1$ is satisfied, the steady state is linearly stable as a solution of (3.39), though Turing diffusion-driven instability phenomena is not exhibited at this state, but with the numerical simulations of the complete system in the presence of diffusion in one-two- and three-dimensions is expected to capture any points and queries that may naturally arise correctly.

4.1. Numerical simulation in one-dimension

In this section, we are expected to capture the theoretical results through numerical experiment of the full diffusive system. We examine our numerical experiment of the time-fractional reaction–diffusion systems (3.39) in just one-dimensional space. To start with, we first check the behaviour of time-fractional index α on the solution of u and v. For all 1D experiments here, we utilized $a = 0.06, b = 0.02, c = 0.5, d = 0.2, D_u = 0.07, Dv = 0.1$, with step size $h = 0.25$ and time-step $\Delta t = 0.1$. We compute the initial state as

```
u0=0.07*(ones(N,1));
v0=0.1*(ones(N,1));
```

so as to mimic the spatiotemporal evolution of nontrial dynamics. The numerical results obtained for some instances of fractional order is shown in Fig. 4. The results in rows 1 to 3 have shown that both species oscillate in phase at some instances of time-fractional power

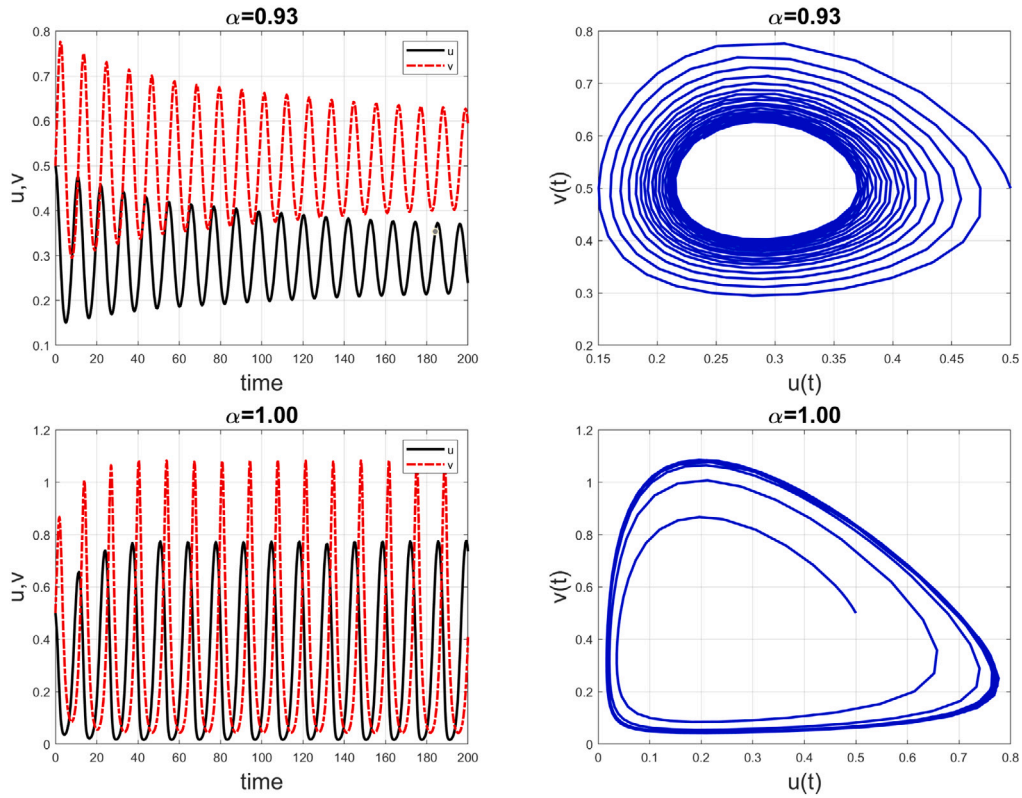

Fig. 3. (a) Phase plane and time-series plots of fractional prey-predator model (3.46) with $\phi = 0.3, \psi = 2$ and $\varphi = 0.8$.

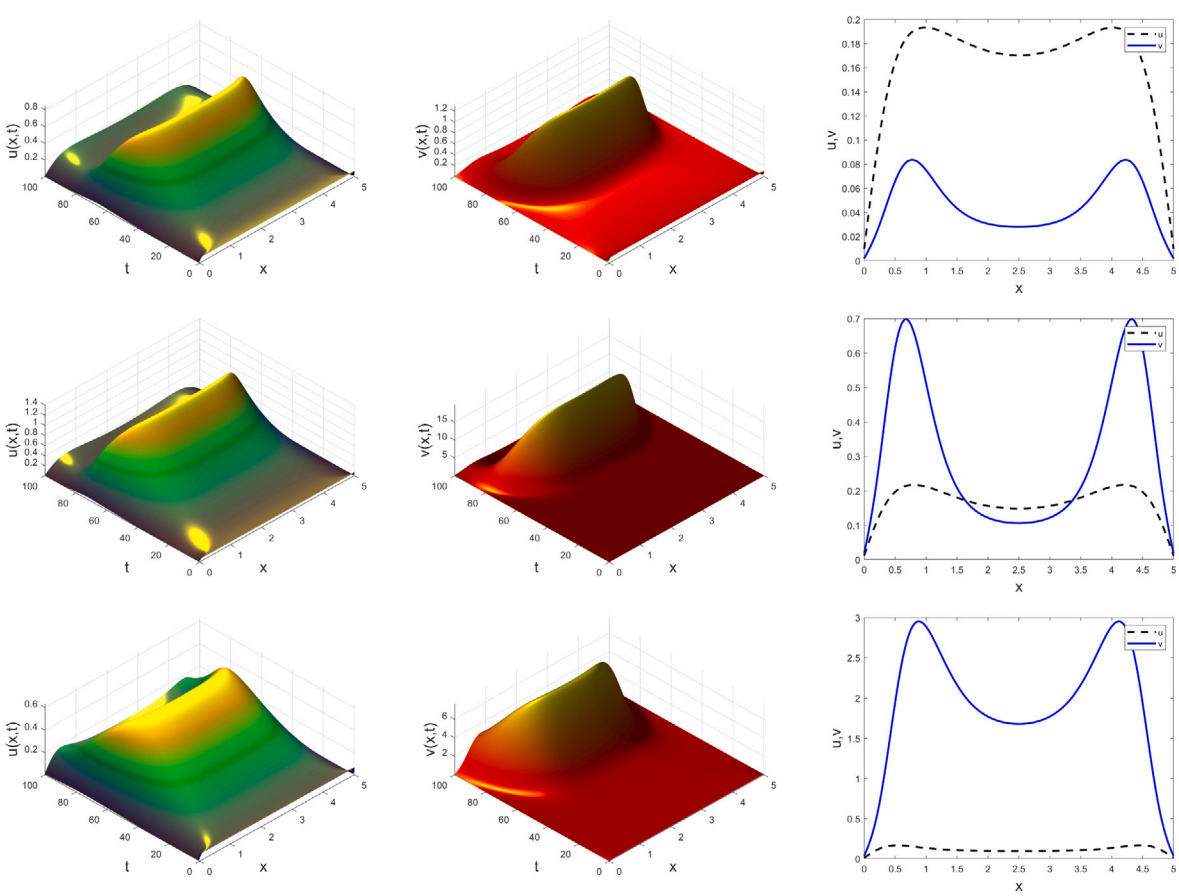

Fig. 4. One-dimensional evolution of fractional predator–prey model (3.39) showing different spatiotemporal evolution of the species for various α.

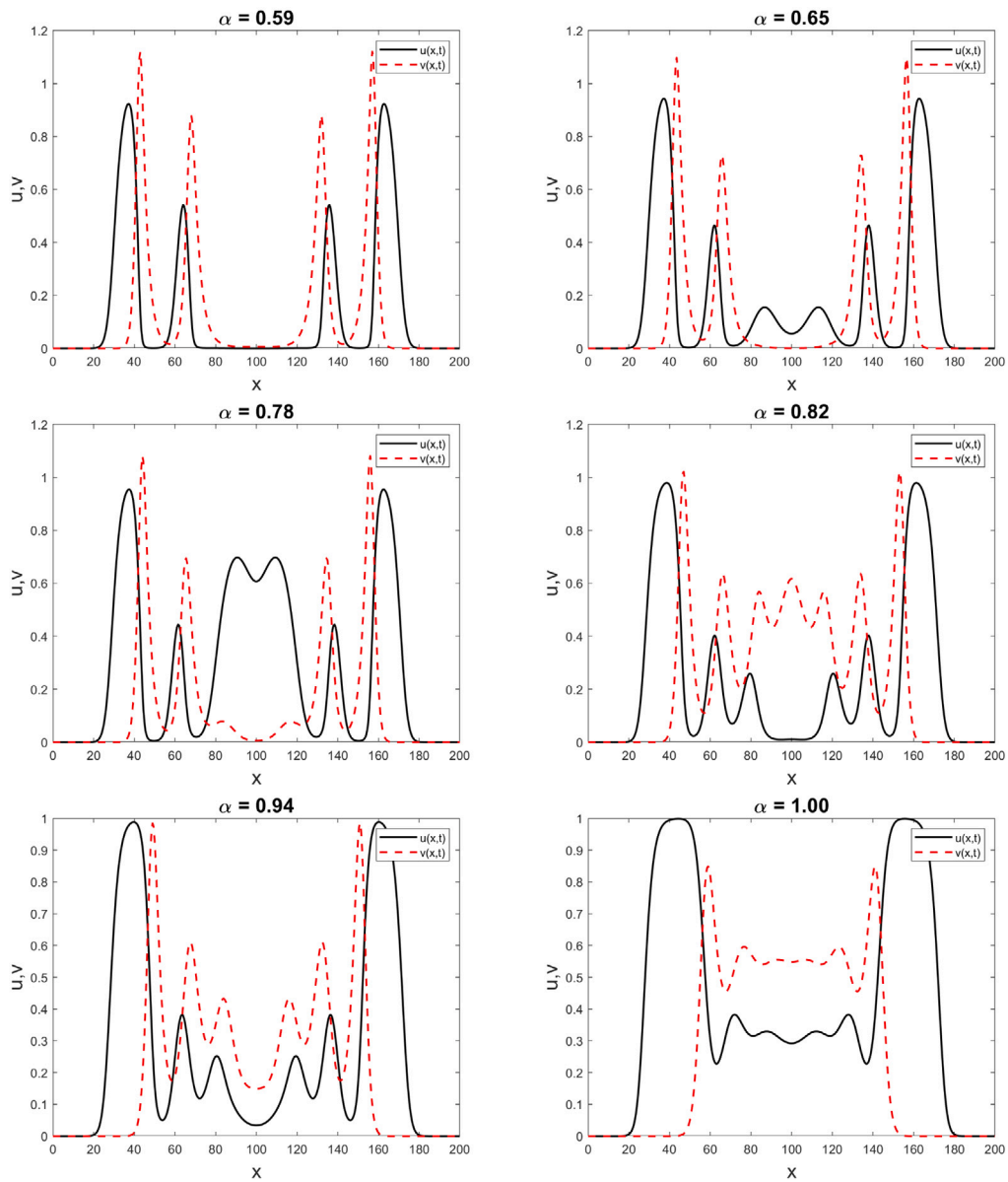

Fig. 5. One-dimensional results of fractional prey-predator model (3.46) with $\phi = 0.3, \psi = 2,\ \varphi = 0.8$ and $\delta = 1.0$ for different α.

α. Rows 1–3 correspond to $\alpha = 0.75, 0.85, 1.00$, respectively. As we can deduce, regardless of the value of α chosen, both species will continue to experience spatiotemporal oscillations. This assertion can also be drawn from the non-spatial model as reported in Fig. 1. It is obvious that both species oscillate more at the neighbourhood of the origin, but as time progress they become stable and permanent. In reality, it means both prey and predator species will continue to coexist in the same habitat.

Similarly, we experiment the predator–prey model (3.43) in one-dimension using the initial data

$$u_0 = \frac{1}{5}\exp(-(x-100)^2), \quad v_0 = v^* \tag{4.51}$$

with $v^* = 0.4$, subject to parameters

$$\phi = 0.3, \psi = 2.0, \varphi = 0.8, \delta = 1.0. \tag{4.52}$$

Effects of fractional-order parameter α is shown in Fig. 5. Effect of φ is verified in Figure Effects of fractional-order parameter α is shown in Fig. 6, and finally we observed the diffusive effect in figure Effects of fractional-order parameter α is shown in Fig. 7. Simulations run for final time $t = 50$.

4.2. Numerical simulations in two-dimension

Numerical experiments in one-dimension is simple to implement. Bear in mind that it is in higher dimensions that the numerical method presented in this paper can really become of important value. The two-variable system of reaction–diffusion model has a lot of delicate features that are not visible in one-dimension, and not easy for a mere scheme to extract.[3–6] This is one of the major motives behind the use of new iterative method in this work. Here, a Neumann (zero-flux) boundary conditions is chosen subject to initial condition[30,62]

$$\begin{aligned} u(x,y,0) &= u^* - (2\times 10^{-7})(x-0.1y-225)(x-0.1y-675), \\ v(x,y,0) &= v^* - (3\times 10^{-5})(x-450) - (1.2\times 10^{-4})(y-150) \end{aligned} \tag{4.53}$$

The choice of using the initial conditions in (4.53) permits us examine the 2D computations in a nontrivial manner as such system is highly unstable in the presence of diffusion. It should be noted that it is important to take domain size L large enough to enable the waves to propagate. To achieve this, we let $x, y \in [0, L] \times [0, L]$ for $L = 400$, $\delta = 0.005$. Different types of dynamical behaviours were displayed in the numerical simulations. Consequently, it was found that the distribution

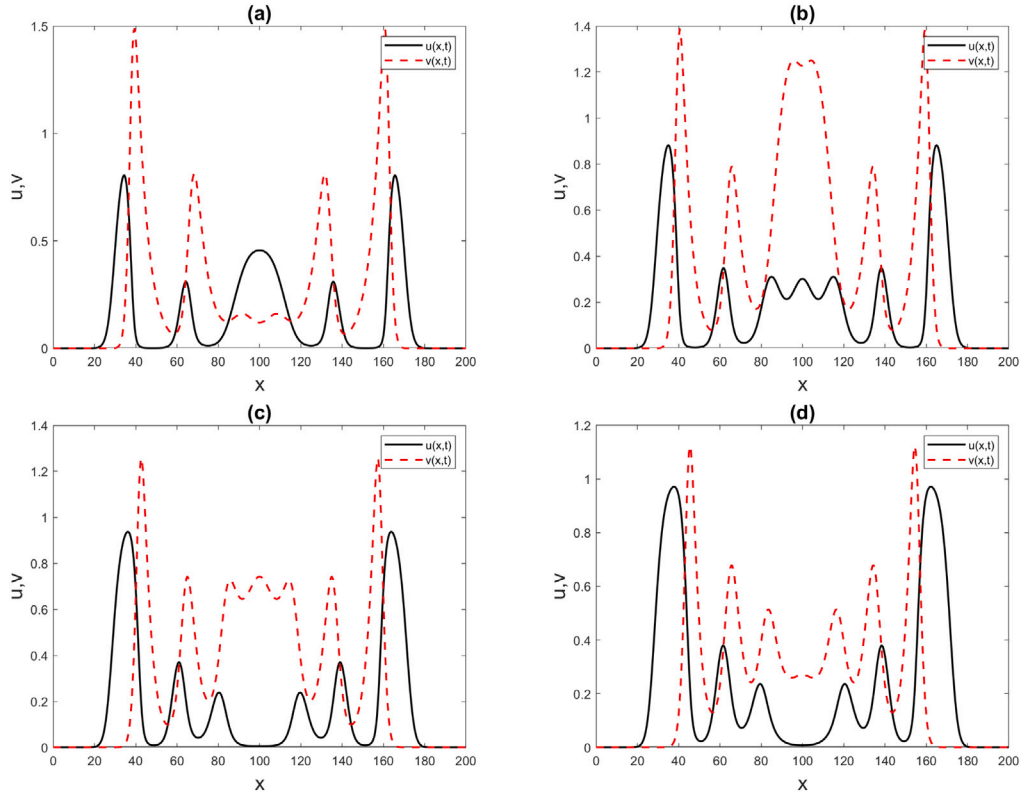

Fig. 6. Spatiotemporal distribution of model (3.46) with various ψ and $\alpha = 0.90$. Plots (a): $\psi = 0.25$, (b): $\psi = 0.5$, (c) $\psi = 1.25$, and (d): $\psi = 1.50$.

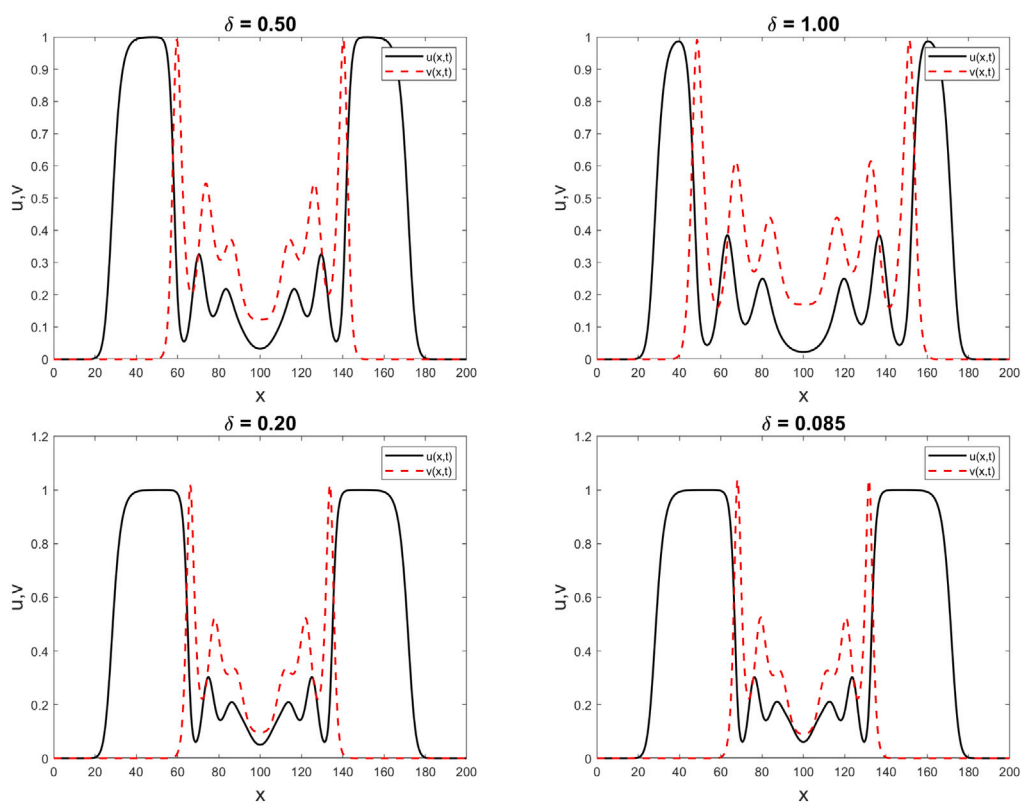

Fig. 7. Spatiotemporal distribution of model (3.46) showing diffusive effects, with fixed $\alpha = 0.81$.

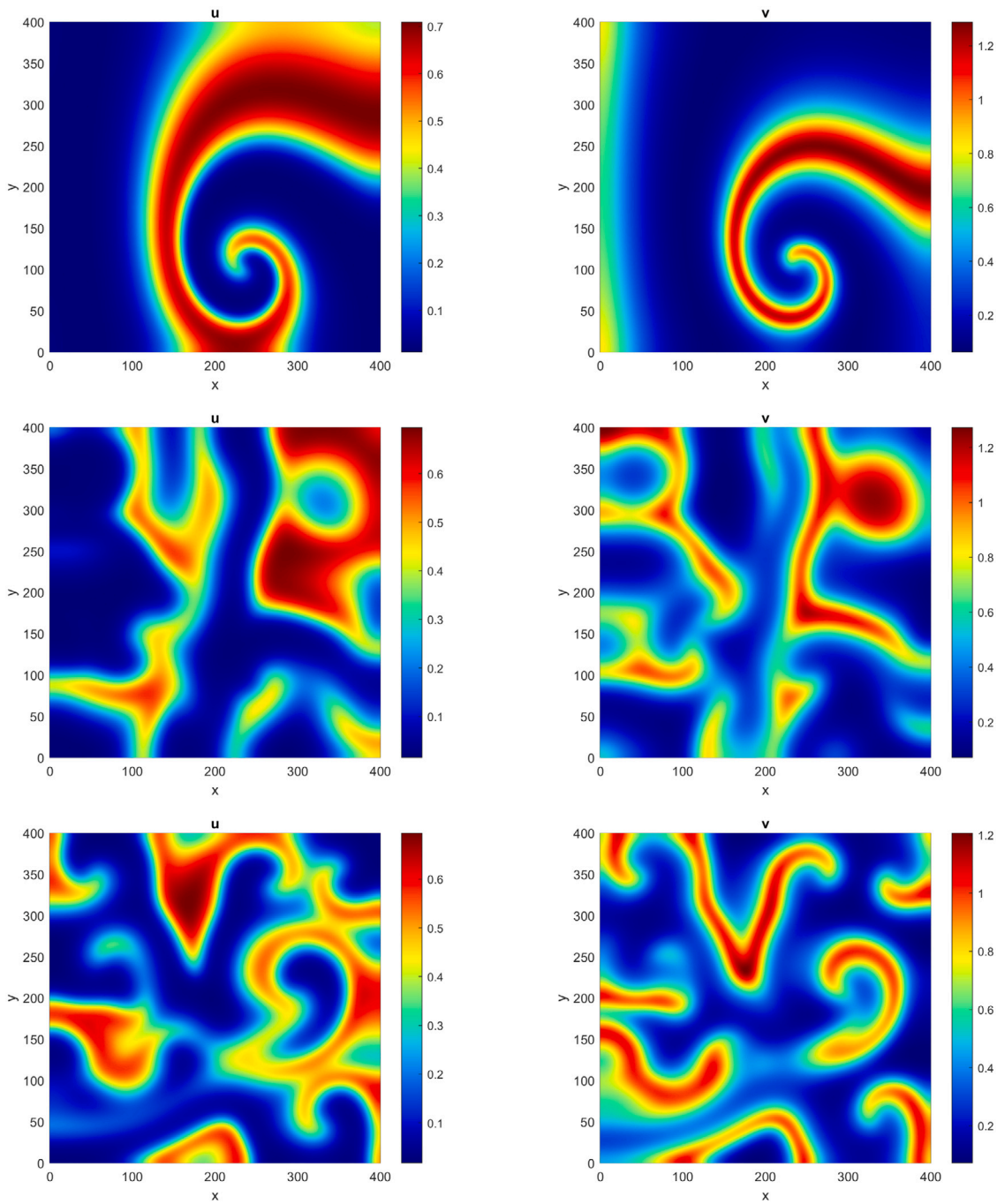

Fig. 8. Two-dimensional evolution of fractional predator–prey system (3.43) with $\alpha = 0.85$. Rows 1, 2 and 3 correspond to varying simulation time $t = 150, t = 1000$ and $t = 1500$, respectively. Other parameters remain as given in (4.52).

of predator and prey are of the same type. Though we decided to carry out the analysis of pattern formation for the distribution of u– and v–species as displayed in Fig. 8 to enable our readers to see the similarities.

In the same manner, we set $\alpha = 0.95$ and increase the simulation time further to obtain the dynamic evolution in Fig. 9. Other parameters are in Eq. (4.52). The two results here show that the interaction between the prey-species and v–species within a given habitat is chaotic. Obviously, regardless of time and variation in parameters, the dynamic behaviour will ever remain as chaotic spirals, this behaviour is in agreement with the known Turing patterns. The thick coloured spiral regions arise from clustering of different isoclines which correspond to the sharp gradients in the predator–prey densities. The population outside the curve is zero. It should be mentioned that other behavioural patterns apart from the ones obtained in this work are possible by varying the choice of initial function fixed here. For certain parameter choices, the kinetics admits a stable limit cycle surrounding the unstable equilibrium point (u^*, v^*), that is, the densities of the two species cycle periodically in time.

4.3. Numerical simulations in three-dimension

Applicability of our numerical method is further tested by giving an extension to the solution of model (3.43) in three-dimensions. In this

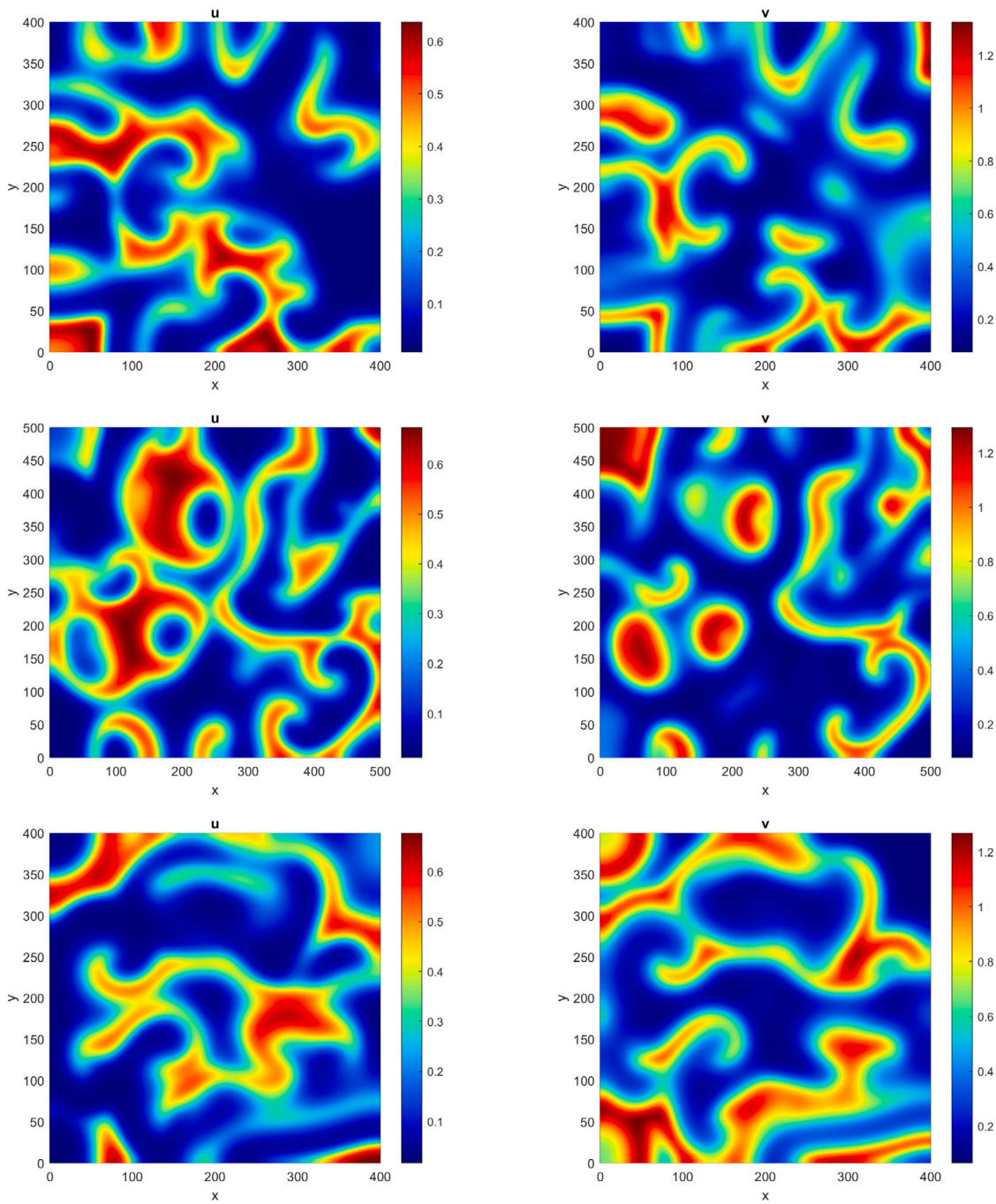

Fig. 9. Two-dimensional evolution of fractional predator–prey system (3.43) with $\alpha = 0.95$. Rows 1, 2 and 3 correspond to varying simulation time $t = 2000, t = 3000$ and $t = 4000$, respectively. Other parameters remain as given in (4.52).

circumstance, we also set the initial conditions to be

$$\begin{aligned} u(x,y,0) &= 1 - 0.5\exp(-50((x-\nu/2)^2 + (y-\nu/2)^2 + (z-\nu/2)^2)), \\ v(x,y,0) &= 0.25\exp(-50((x-\nu/2)^2 + (y-\nu/2)^2 + (z-\nu/2)^2)) \end{aligned} \tag{4.54}$$

We equally apply the Neumann (zero-flux) boundary clamped at the ends of domain size $x, y, z \in [-L, L]\times[-L, L]\times[-L, L]$ for $L = 10$. A 3D surface plot illustrating the type of patterns that can arise by diffusion-driven instabilities are shown in Figs. 10 and 11 for different α at final simulation time $t = 200$. These are typical patterns for a two-variable reaction–diffusion model that represents the interaction between a prey and predator species, moving through a diffusion process. So the patterns obtained here are purely based on the species interactions and not by any underlying heterogeneity in the domain. The main pattern formed, that is strips or cone-like pattern, subjects to the domain size in which species live and on the control parameter $0 \le \alpha \le 1$ and the diffusion rate.

5. Conclusion

In this paper, we have examined the richness of spatiotemporal phenomena of an important dynamic of the diffusive predator–prey systems. We investigate the Turing stability analysis of the models via the linear stability analysis. Apart from the analytical study of such models, we present the Laplace transform-homotopy method to perform the direct numerical simulation of the diffusive system without necessarily going through the rigors of spatial discretization. The results

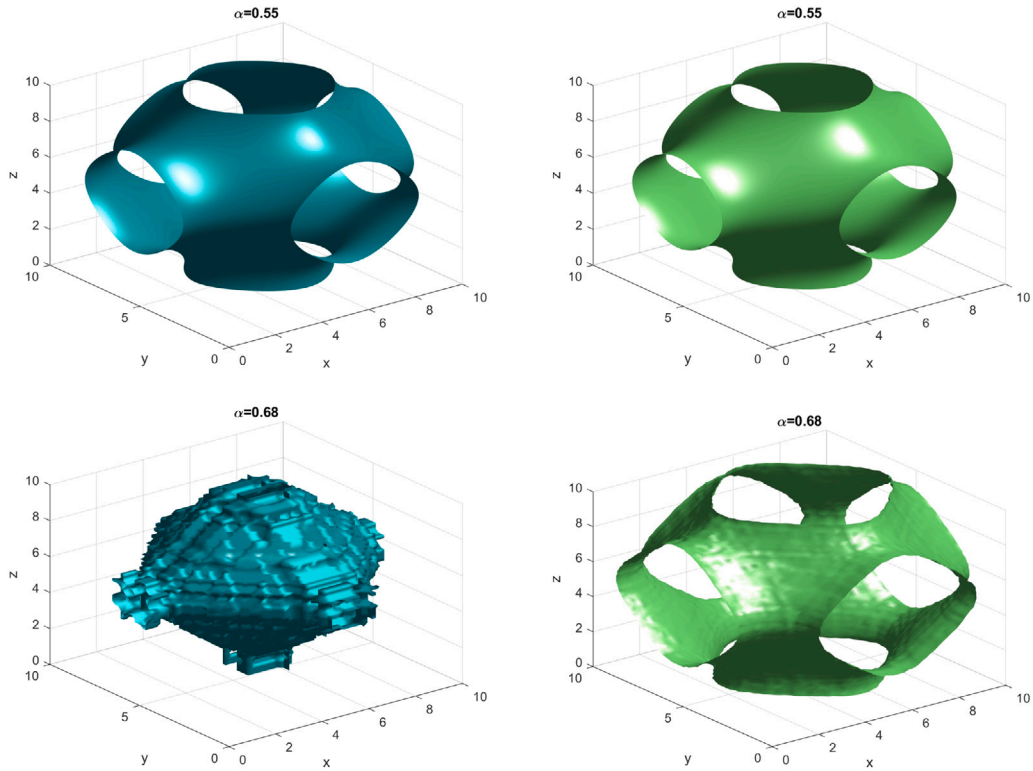

Fig. 10. (a) Numerical solution of predator–prey system (3.43) in three dimensions at $\phi = 0.3$, $\psi = 2$ and $\varphi = 0.8$, $\delta = 0.045$.

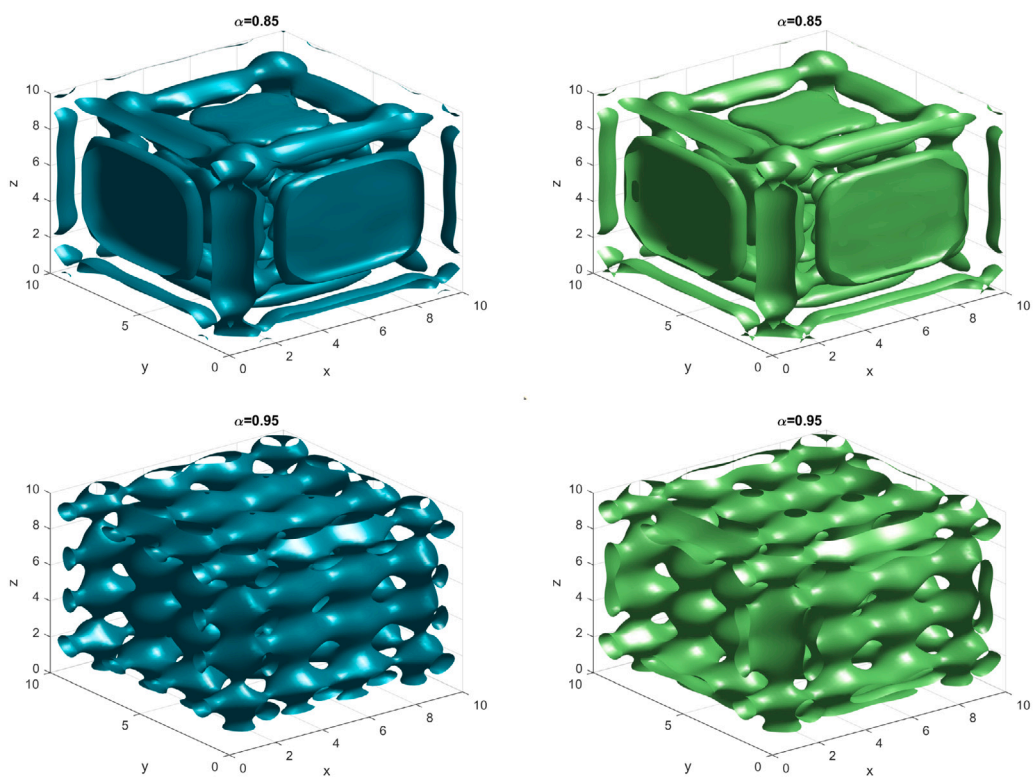

Fig. 11. (a) Numerical solution of predator–prey system (3.43) in three dimensions at $\phi = 0.28$, $\psi = 1.65$ and $\varphi = 0.8$, $\delta = 0.045$.

presented in this paper are ecologically meaningful with the hope that they will be useful for studying the spatiotemporal phenomena arising in mathematical ecology. The new mathematical approach presented in this work can be extended to seek the appropriate numerical solution of any higher dimensional reaction–diffusion of physical and practical problems. Also, the present can be applied to the pattern formation process in subdiffusive and superdiffusive predator–prey dynamics.

Declaration of competing interest

The authors declare that they have no known competing financial interests or personal relationships that could have appeared to influence the work reported in this paper.

Data availability

No data was used for the research described in the article.

References

1. Das S. *Functional Fractional Calculus for System Identification and Controls*. New York: Springer; 2008.
2. Kilbas AA, et al *Theory and Applications of Fractional Differential Equations*. San Diego: Elsevier; 2006.
3. Owolabi KM. Numerical simulation of fractional-order reaction–diffusion equations with the Riesz and Caputo derivatives. *Neural Comput Appl*. 2019;34:4093–4104. http://dx.doi.org/10.1007/s00521-019-04350-2.
4. Owolabi KM. Numerical approach to chaotic pattern formation in diffusive predator–prey system with Caputo fractional operator. *Numer Methods Partial Differ Equ*. 2020:1–21. http://dx.doi.org/10.1002/num.22522.
5. Owolabi KM, et al Dynamics of pattern formation process in fractional-order super-diffusive processes: A computational approach. *Soft Comput*. 2021;25:11191–11208. http://dx.doi.org/10.1007/s00500-021-05885-0.
6. Owolabi KM, Baleanu D. Emergent patterns in diffusive Turing-like systems with fractional-order operator. *Neural Comput Appl*. 2021;33:12703–12720. http://dx.doi.org/10.1007/s00521-021-05917-8.
7. Podlubny I. *Fractional Differential Equations*. San Diego: Academic Press; 1999.
8. Samko S, Kilbas A, Marichev O. *Fractional Integrals and Derivatives: Theory and Applications*. Amsterdam: Gordon and Breach; 1993.
9. Agarwal P, Singh R. Modelling of transmission dynamics of Nipah virus (niv): A fractional order Approach. *Phys A*. 2020;547:124243. http://dx.doi.org/10.1016/j.physa.2020.124243.
10. Baleanu D, Ghassabzade FA, Nieto JJ, Jajarmi A. On a new and generalized fractional model for a real cholera outbreak. *Alex Eng J*. 2022;61:9175–9186.
11. ul Rehman A, Singh R, P. Agarwal. Modeling, analysis and prediction of new variants of covid-19 and dengue co-infection on complex network. *Chaos Solitons Fractals*. 2021;150:111008. http://dx.doi.org/10.1016/j.chaos.2021.111008.
12. ul Rehman A, Singh R, Abdeljawad T, Okyere E, Guran L. Modeling, analysis and numerical solution to malaria fractional model with temporary immunity and relapse. *Adv Differential Equations*. 2021;390:2021. http://dx.doi.org/10.1186/s13662-021-03532-4.
13. Sharma N, Singh R, Singh J, Castillo O. Modeling assumptions, optimal control strategies and mitigation through vaccination to Zika virus. *Chaos Solitons Fractals*. 2021;15:111137. http://dx.doi.org/10.1016/j.chaos.2021.111137.
14. Anthony W, Leung AW. *Nonlinear Systems of Partial Differential Equations, Applications to Life and Applied Sciences*. Singapore: World Scientific Publishing; 2009.
15. Chang Y, et al Permanence and coexistence in a diffusive complex ratio-dependent food chain. *Int J Dyn Control*. 2015;3:262–274. http://dx.doi.org/10.1007/s40435-014-0131-4.
16. Feng W, et al Global attractors of reaction–diffusion systems modeling food chain populations with delays. *Commun Pure Appl Anal*. 2011;10:1463–1478. http://dx.doi.org/10.3934/cpaa.2011.10.1463.
17. Roose T, Chapman SJ, Maini PK. Mathematical models of avascular tumor growth. *SIAM Rev*. 2007;9:179–208. http://dx.doi.org/10.1137/S0036144504446291.
18. Lotka AJ. *The Elements of Physical Biology*. Baltimore: Williams and Wilkins; 1952.
19. Volterra V. Fluctuation in abundance of the species considered mathematically. *Nature*. 1926;118:558–560. http://dx.doi.org/10.1038/118558a0.
20. Volterra V. *Variations and Fluctuations of the Numbers of Individuals in Animal and Species Living Together*. New York: McGraw-Hill; 1926 Reprinted in 1931 in R.N. Chapman, Animal Ecology.
21. Mondal B, et al Complex dynamics of a generalist predator–prey model with hunting cooperation in predator. *Eur Phys J Plus*. 2022;137:43. http://dx.doi.org/10.1140/epjp/s13360-021-02272-4.
22. Patra RR, et al Effect of delay and control on a predator–prey ecosystem with generalist predator and group defence in the prey species. *Eur Phys J Plus*. 2022;137:28. http://dx.doi.org/10.1140/epjp/s13360-021-02225-x.
23. Paul P, et al Reactivity in prey–predator models at equilibrium under selective harvesting efforts. *Eur Phys J Plus*. 2021;136:510. http://dx.doi.org/10.1140/epjp/s13360-021-01525-6.
24. Rajni, Ghosh B. Multistability, chaos and mean population density in a discrete-time predator–prey system. *Chaos Solitons Fractals*. 2022;162:112497. http://dx.doi.org/10.1016/j.chaos.2022.112497.
25. Shivam K, et al Untangling role of cooperative hunting among predators and herd behavior in prey with a dynamical systems approach. *Chaos Solitons Fractals*. 2022;162:112420. http://dx.doi.org/10.1016/j.chaos.2022.112420.
26. Sun G, et al Predator cannibalisms can give rise to regular spatial patterns in a predator–prey system. *Nonlinear Dynam*. 2009;58:75–84. http://dx.doi.org/10.1007/s11071-008-9462-z.
27. Allen LJS. *An Introduction to Mathematical Biology*. New Jersey: Pearson Education. Inc.; 2007.
28. Alonso D, et al Mutual interference between predators can give rise to Turing spatial patterns. *Ecology*. 2002;83:28–34. http://dx.doi.org/10.2307/2680118.
29. Boukal DS, et al How predator functional responses and Allee effects in prey affect the paradox of enrichment and population collapses. *Theor Popul Biol*. 2007:136–147. http://dx.doi.org/10.1016/j.tpb.2006.12.003.
30. Garvie MR. Finite-difference schemes for reaction–diffusion equations modeling predator-pray interactions in MATLAB. *Bull Math Biol*. 2007;69:931–956. http://dx.doi.org/10.1007/s11538-006-9062-3.
31. Daftardar-Gejji V, Jafari H. An iterative method for solving nonlinear functional equations. *J Math Anal Appl*. 2006;316(2):753–763. http://dx.doi.org/10.1016/j.jmaa.2005.05.009.
32. He JH. Homotopy perturbation technique. *Comput Methods Appl Mech Engrg*. 1999;178(3):257–262. http://dx.doi.org/10.1016/S0045-7825(99)00018-3.
33. Ray SS, Bera RK. Solution of an extraordinary differential equation by Adomian decomposition method. *J Appl Math*. 2004;4:331–338. http://dx.doi.org/10.1155/S1110757X04311010.
34. Dehghan M, et al Solving nonlinear fractional partial differential equations using the homotopy analysis method. *Numer Methods Partial Differ Equ*. 2010;26(2):448–479. http://dx.doi.org/10.1002/num.20460.
35. Odibat Z, et al A reliable algorithm of homotopy analysis method for solving nonlinear fractional differential equations. *Appl Math Model*. 2010;34(3):593–600. http://dx.doi.org/10.1016/j.apm.2009.06.025.
36. Hemeda AA. Homotopy perturbation method for solving partial differential equations of fractional order. *J Math Anal*. 2012;6(49–52):2431–2448. http://dx.doi.org/10.1155/2014/594245.
37. Hemeda AA. Homotopy perturbation method for solving systems of nonlinear coupled equations. *Appl Math Sci*. 2012;6(93–96):4787–4800.
38. Sakar MG, et al Variational iteration method for the time-fractional Fornberg-Whitham equation. *Comput Math Appl*. 2012;63(9):1382–1388. http://dx.doi.org/10.1016/j.camwa.2012.01.031.
39. Doha EH, et al Efficient Chebyshev spectral methods for solving multi-term fractional orders differential equations. *Appl Math Model*. 2011;35(12):5662–5672. http://dx.doi.org/10.1016/j.apm.2011.05.011.
40. Doha EH, et al A Chebyshev spectral method based on operational matrix for initial and boundary value problems of fractional order. *Comput Math Appl*. 2011;62(5):2364–2373. http://dx.doi.org/10.1016/j.camwa.2011.07.024.
41. Aminikhah H. The combined Laplace transform and new homotopy perturbation methods for stiff systems of ODEs. *Appl Math Model*. 2012;36:3638–3644. http://dx.doi.org/10.1016/j.apm.2011.10.014.
42. Kamdem JS. Generalized integral transforms with the homotopy perturbation method. *Math Model Algorithms Oper Res*. 2014;13(2):209–232. http://dx.doi.org/10.1007/s10852-013-9232-x.
43. Miller K, Ross B. *An Introduction to the Fractional Calculus and Fractional Differential Equations*. New York: John Wiley & Sons Inc.; 1993.
44. Datsko B, et al Pattern formation in fractional reaction–diffusion systems with multiple homogeneous states. *Int J Bifurc Chaos Appl Sci Eng*. 2012;22:1250087. http://dx.doi.org/10.1142/S0218127412500873.
45. Aktar MS, et al Spatio-temporal dynamic solitary wave solutions and diffusion effects to the nonlinear diffusive predator–prey system and the diffusion-reaction equations. *Chaos Solitons Fractals*. 2022;160:112212. http://dx.doi.org/10.1016/j.chaos.2022.112212.
46. Bi Z, et al Spatial dynamics of a fractional predator–prey system with time delay and Allee effect. *Chaos Solitons Fractals*. 2022;162:112434. http://dx.doi.org/10.1016/j.chaos.2022.112434.
47. Chen M, Zheng Q. Predator-taxis creates spatial pattern of a predator–prey model. *Chaos Solitons Fractals*. 2022;161:112332. http://dx.doi.org/10.1016/j.chaos.2022.112332.
48. Kaviya R, Muthukumar P. Dynamical analysis and optimal harvesting of conformable fractional prey–predator system with predator immigration. *Eur Phys J Plus*. 2021;136:542. http://dx.doi.org/10.1140/epjp/s13360-021-01559-w.
49. Han B, Jiang D. Stationary distribution, extinction and density function of a stochastic prey-predator system with general anti-predator behavior and fear effect. *Chaos Solitons Fractals*. 2022;162:112458. http://dx.doi.org/10.1016/j.chaos.2022.112458.

50. Owolabi KM. Computational study for the Caputo sub-diffusive and Riesz super-diffusive processes with a fractional order reaction–diffusion equation. *Partial Differ Equ Appl Math*. 2023:100564. http://dx.doi.org/10.1016/j.padiff.2023.100564.
51. Odibat Z, Shawagfeh N. Generalized Taylor's formula. *Appl Math Comput*. 2007;186:286–293. http://dx.doi.org/10.1016/j.amc.2006.07.102.
52. Yu R, Zhang H. New function of Mittag-Leffler type and its application in the fractional diffusion-wave equation. *Chaos Solitons Fractals*. 2006;30:946–955. http://dx.doi.org/10.1155/2013/454209.
53. Murray JD. *Mathematical Biology II: Spatial Models and Biomedical Applications*. Berlin: Springer-Verlag; 2003.
54. Murray JD. *Mathematical Biology I: An Introduction*. New York: Springer-Verlag; 2002.
55. Petrovskii S, et al Allee effect makes possible patchy invasion in a predator–prey system. *Ecol Lett*. 2002;5:345–352. http://dx.doi.org/10.1046/j.1461-0248.2002.00324.x.
56. Owolabi KM, Patidar KC. Numerical simulations of multicomponent ecological models with adaptive methods. *Theor Biol Med Model*. 2016;13:1. http://dx.doi.org/10.1186/s12976-016-0027-4.
57. Alqhtani M, et al Spatiotemporal (target) patterns in sub-diffusive predator–prey system with the Caputo operator. *Chaos Solitons Fractals*. 2022;160:112267. http://dx.doi.org/10.1016/j.chaos.2022.112267.
58. Alqhtani M, et al Efficient numerical techniques for computing the Riesz fractional-order reaction–diffusion models arising in biology. *Chaos Solitons Fractals*. 2022;161:112394. http://dx.doi.org/10.1016/j.chaos.2022.112394.
59. Medvinsky A, et al Spatiotemporal complexity of plankton and fish dynamics. *SIAM Rev*. 2002;44:311–370. http://dx.doi.org/10.1137/S0036144502404442.
60. Owolabi KM, Patidar KC. Numerical solution of singular patterns in one-dimensional Gray-Scott-like models. *Int J Nonlinear Sci Numer*. 2014;15:437–462. http://dx.doi.org/10.1515/ijnsns-2013-0124.
61. Owolabi KM, Patidar KC. Higher-order time-stepping methods for time-dependent reaction–diffusion equations arising in biology. *Appl Math Comput*. 2014;240:30–50. http://dx.doi.org/10.1016/j.amc.2014.04.055.
62. Owolabi KM. Robust IMEX schemes for solving two-dimensional reaction–diffusion models. *Int J Nonlinear Sci Numer Simul*. 2015;16:271–284. http://dx.doi.org/10.1515/ijnsns-2015-0004.
63. Wang M, et al Complex patterns in a predator–prey system with self and cross-diffusion. *Commun Nonlinear Sci Numer Simul*. 2011;16:2006–2015. http://dx.doi.org/10.1016/j.cnsns.2010.08.035.
64. Wang MW, et al Pattern selection in a predation model with self and cross-diffusion. *Chin Phys D*. 2011;20:034702. http://dx.doi.org/10.1088/1674-1056/20/3/034702.
65. Xue L. Pattern formation in a predator–prey model with spatial effect. *Phys A*. 2012;391:5987–5996. http://dx.doi.org/10.1016/j.physa.2012.06.029.
66. Yang B. Pattern formation in a diffusive ratio-dependent Holling-Tanner predator–prey model with Smith growth. *Discrete Dyn Nat Soc*. 2013:454209. http://dx.doi.org/10.1155/2013/454209, 1-8.